ASEAN Engineering Journal

Full Paper

FEASIBILITY ANALYSIS OF HYDROGEN-FREE DEOXYGENATION REACTIONS OF PALMITIC ACID TO HYDROCARBONS FUELS THROUGH THERMODYNAMIC STUDIES

Article history
Received
29 March 2023
Received in revised form
15 August 2023
Accepted
24 August 2023
Published online
29 February 2024

Teguh Riyanto[a,b], I. Istadi[a,b]*, Didi D. Anggoro[b], Bunjerd Jongsomjit[c]

[a]Laboratory of Plasma-Catalysis (R3.5), Center of Research and Services - Diponegoro University (CORES-DU), Integrated Laboratory, Universitas Diponegoro, Semarang, Central Java 50275, Indonesia
[b]Department of Chemical Engineering, Faculty of Engineering, Universitas Diponegoro, Semarang, Central Java 50275, Indonesia
[c]Department of Chemical Engineering, Faculty of Engineering, Chulalongkorn University, Bangkok 10330, Thailand

*Corresponding author
istadi@che.undip.ac.id

Graphical abstract

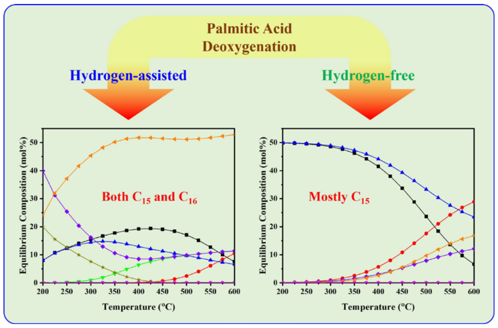

Abstract

Four models were investigated to study the feasibility of the hydrogen-free deoxygenation of palmitic acid to hydrocarbons through the stoichiometric thermodynamic equilibrium analysis. The reaction conditions have been varied to estimate the equilibrium reactions composition (temperature (T) of 200 – 600 °C, pressure (P) of 1 – 20 bar, and H_2/Palmitic acid ratio of 0 – 10). It was found that the hydrogen-free deoxygenation of palmitic acid was thermodynamically favorable with complete conversion (≈100%) at all investigated reaction conditions. The equilibrium products composition was significantly affected by reaction temperature. The main-formed hydrocarbon was $C_{15}H_{32}$ at low temperatures and $C_{15}H_{30}$ at high temperatures. However, the product composition of reaction equilibrium was not affected by the reaction pressure. Even though the internal hydrogen was generated, the hydrodeoxygenation reaction pathways were not too favorable because the hydrodeoxygenation product and its intermediates were negligible.

Keywords: Hydrogen-free deoxygenation; Palmitic acid; Thermodynamic analysis; Feasibility study

1.0 INTRODUCTION

Lately, biofuels have been highly developed by most researchers around the world due to the limitation of fossil-based fuels. Biofuels are generated from biomass, such as cellulose-based [1–3] and oil-based [4–6] feedstocks, through appropriate chemical processes. Several researchers have reported the thermal processing of cellulose-based feedstocks to produce biofuels in which oxygenated and aromatic compounds are found to be dominant in the biofuels product [1,2,7]. The aromatic compounds are needed in gasoline-range biofuels to increase their octane number [8]. However, these compounds should be limited, because they can be released into the environment as toxic compounds during the combustion process [9]. On the other hand, the conversion of oil-based biomass is more promising than cellulose-based, because it is composed of linear hydrocarbons.

The most developed oil-based biomass is vegetable oil, which mainly contains triglyceride and its derived components, i.e. fatty acids [10–12]. Many processes have been studied to produce biofuels from vegetable oil and its derived components, including pyrolysis and catalytic cracking. However, the main problem with those processes is that the produced biofuels still contain oxygenated compounds, which can reduce the heat capacity or heating value [8]. Therefore, many researchers focused on the deoxygenation process to eliminate or reduce the oxygen content in biofuels [13–15].

Other than reducing the oxygen content of biofuels, many researchers deoxygenated the vegetable oil or its derived components to produce diesel-range hydrocarbons. Istadi *et al.* [16] converted palm oil, as a natural source of triglyceride, to low-oxygenated biofuels at the presence of hydrogen using the acid-treated spent residue fluid catalytic cracking (RFCC) catalysts. Previously, Loe *et al.* [17] reported the hydrodeoxygenation of some model compounds, namely triolein, tristearin, and stearic acid. With respect to the conversion of model compounds, Loe *et al.* [18] converted tristearin to diesel-range hydrocarbons under the hydrogen atmosphere using Pt-promoted Ni-based catalysts, in which the main products were C_{17}-hydrocarbons. In addition, Lestari *et al.* [19] conducted the deoxygenation of saturated fatty acids, namely palmitic acid (C_{16}-saturated fatty acid) and stearic acid (C_{18}-saturated fatty acid), using palladium-based catalysts under the presence of diluted-hydrogen (5% in Ar) at 17 bar. They reported that the main reaction products were C_{15}- and C_{17}-aliphatic hydrocarbons.

Many researchers conducted the deoxygenation of triglycerides or fatty acids under the presence of hydrogen or by introducing external hydrogen to the reaction system. The main goal of introducing hydrogen to the deoxygenation reaction system is to eliminate the oxygen atom from the feedstock. Furthermore, the deoxygenation reaction may produce biofuels with high combustion efficiency because of the high carbon and hydrogen content in the biofuels [20]. However, the utilization of external hydrogen lies down in an uneconomical process, because of uneconomically viable of expensive hydrogen.

It has been postulated that the hydrogen-free deoxygenation pathways, namely decarboxylation and decarbonylation reactions, can occur during the hydrodeoxygenation process [19,21–23]. Therefore, converting triglycerides or fatty acids to hydrocarbons via hydrogen-free deoxygenation is expected to be possibly conducted. However, its feasibility should be studied from the thermodynamic point of view to determine the possible operating condition as well as the composition of the products. Thermodynamic equilibrium analysis is a valuable tool for investigating the feasibility of reactions. This study comprehensively analyzes the feasibility of hydrogen-free deoxygenation reactions of palmitic acid, as a model compound. To the best of our knowledge, comprehensive thermodynamic equilibrium analysis of palmitic acid conversion through hydrogen-free deoxygenation reactions has not studied yet. Therefore, this study aims to evaluate the feasibility of hydrogen-free and hydrogen-assisted deoxygenation of palmitic acid to produce hydrocarbons based on stoichiometric thermodynamic equilibrium. Some recommendations for further experimental study are also given in the last part of this study based on the assumption that the reactions are thermodynamically controlled and not kinetically controlled.

2.0 METHOD

2.1 Reaction Pathways of Palmitic Acid Deoxygenation

The deoxygenation reaction of palmitic acid can occur with or without external hydrogen (H_2) gas. In case of no external hydrogen gas is introduced, the reaction may take place in decarboxylation (Equation (1)) and decarbonylation (Equation (2)) reactions as follows:

$$C_{16}H_{32}O_2 \rightarrow C_{15}H_{32} + CO_2 \quad \Delta H^0_{298K} = -9.26 \text{ kJ/mol} ; \Delta G^0_{298K} = -60.11 \text{ kJ/mol} \tag{1}$$

$$C_{16}H_{32}O_2 \rightarrow C_{15}H_{30} + CO + H_2O \quad \Delta H^0_{298K} = +157.43 \text{ kJ/mol} ; \Delta G^0_{298K} = +53.28 \text{ kJ/mol} \tag{2}$$

The decarboxylation reaction of palmitic acid produces saturated hydrocarbon with one carbon shorter than palmitic acid (Equation (1)), while oxygen atom is released from palmitic acid as CO_2 molecule (decarboxylation). On the other hand, the decarbonylation reaction of palmitic acid produces unsaturated hydrocarbon with one carbon shorter than palmitic acid by releasing oxygen atom as CO and H_2O (Equation (2)).

In case of external hydrogen gas is added to the reaction system, the deoxygenation of palmitic acid takes place in hydro-decarbonylation (Equation (3)) and hydrodeoxygenation (Equation (4)) as follows:

$$C_{16}H_{32}O_2 + H_2 \rightarrow C_{15}H_{32} + CO + H_2O \quad \Delta H^0_{298K} = +31.91 \text{ kJ/mol} ; \Delta G^0_{298K} = -31.46 \text{ kJ/mol} \tag{3}$$

$$C_{16}H_{32}O_2 + 3H_2 \rightarrow C_{16}H_{34} + 2H_2O \quad \Delta H^0_{298K} = -119.94 \text{ kJ/mol} ; \Delta G^0_{298K} = -114.99 \text{ kJ/mol} \tag{4}$$

In the hydrogen-assisted deoxygenations, including hydro-decarbonylation (Equation (3)) and hydrodeoxygenation (Equation (4)) reactions, the palmitic acid is converted into saturated hydrocarbons, (n-pentadecane, CO, and H_2O). Besides, palmitic acid is also converted into n-hexadecane and H_2O. In fact, the hydrocarbons chain from hydrodeoxygenation is longer than that from hydro-decarbonylation, highly showing the stoichiometric ratio of hydrogen to palmitic acid.

Both hydrogen-free deoxygenation and hydrogen-assisted deoxygenation reactions release CO and H_2O as the byproducts. Therefore, the water gas shift (WGS) reaction (Equation (5)) may occur during the deoxygenation process. Through the WGS reaction, internal hydrogen gas can be generated, even in hydrogen-free deoxygenation.

$$CO + H_2O \leftrightarrow CO_2 + H_2 \quad \Delta H^0_{298K} = -41.17 \text{ kJ/mol} ; \Delta G^0_{298K} = -28.65 \text{ kJ/mol} \tag{5}$$

Concerning the hydrodeoxygenation reaction of palmitic acid, the conversion of palmitic acid into n-hexadecane has been reported to pass through the intermediate species, namely hexadecanal and hexadecanol [24,25]. It can be seen in Equation (4) that the hydrogen-assisted decarbonylation needs three moles of hydrogen stoichiometrically to convert palmitic acid into n-hexadecane. The first hydrogenation converts palmitic acid to hexadecanal by releasing one mol of H_2O (Equation (6)). The hydrogenation of the hexadecanal produces hexadecanol (Equation (7)), which can further be hydrogenated into n-hexadecane (Equation (8)) or dehydrated into 1-hexadecene (Equation (9)) [26,27].

$$C_{16}H_{32}O_2 + H_2 \rightarrow C_{16}H_{32}O + H_2O \quad \Delta H^0_{298K} = +36.05 \text{ kJ/mol} ; \Delta G^0_{298K} = +10.29 \text{ kJ/mol} \tag{6}$$

$$C_{16}H_{32}O + H_2 \rightarrow C_{16}H_{33}OH \quad \Delta H^0_{298K} = -66.11 \text{ kJ/mol} ; \Delta G^0_{298K} = -28.50 \text{ kJ/mol} \tag{7}$$

$$C_{16}H_{33}OH + H_2 \rightarrow C_{16}H_{34} + H_2O \quad \Delta H^0_{298K} = +151.92 \text{ kJ/mol} ; \Delta G^0_{298K} = -96.77 \text{ kJ/mol} \tag{8}$$

$$C_{16}H_{33}OH \rightarrow C_{16}H_{32} + H_2O \qquad (9)$$
$$\Delta H^0_{298K} = +35.64 \text{ kJ/mol} ;\ \Delta G^0_{298K} = -11.38 \text{ kJ/mol}$$

2.2 Reaction Equilibrium Calculation Method

It is well known that the chemical components of a chemical reaction at equilibrium can be estimated by minimizing the total Gibbs energy of the reaction. Considering that the system contains n mol components, the total Gibbs energy can be estimated using the following property relations (Equations (10) and (11)) [28]:

$$d(nG) = (nV)dP - (nS)dT + \sum_i v_i \mu_i d\varepsilon \qquad (10)$$

$$\sum_i v_i \mu_i = \left[\frac{\partial(nG)}{\partial\varepsilon}\right]_{T,P} = \left[\frac{\partial G^t}{\partial\varepsilon}\right]_{T,P} \qquad (11)$$

where, ε is the reaction coordinate, G^t is the total Gibbs energy, v_i is the stoichiometric coefficient of species i, and μ_i is the chemical potential. In this case, $\sum_i v_i \mu_i$ represents the rate of change of the total Gibbs energy of the system with the reaction coordinate at constant T and P. At the equilibrium, the total Gibbs energy is minimum; therefore, the right term of Equation (11) goes to zero and Equation (11) becomes Equation (12). This equation is further known as the criterion of chemical reaction equilibrium.

$$\sum_i v_i \mu_i = 0 \qquad (12)$$

Substituting the definition of fugacity of a species in solution, the difference of chemical potential (μ_i) and standard Gibbs energy (G_i^o)gain Equation (13), in which $\hat{f}_i$ and f_i^o stand for the fugacity of species i in solution and its standard state, respectively.

$$\mu_i - G_i^o = RT \ln \frac{\hat{f}_i}{f_i^o} \qquad (13)$$

Substituting Equation (13) to Equation (12) obtains Equation (14) to eliminate μ_i. Further solution of Equation (14) results in Equations (15) and (16), while K stands for the equilibrium constant.

$$\sum_i v_i \left[G_i^o + RT \ln \frac{\hat{f}_i}{f_i^o}\right] = 0 \qquad (14)$$

$$\ln \prod_i \left(\frac{\hat{f}_i}{f_i^o}\right)^{v_i} = \frac{-\sum_i v_i G_i^o}{RT} \qquad (15)$$

$$\prod_i \left(\frac{\hat{f}_i}{f_i^o}\right)^{v_i} = \exp\left(\frac{-\Delta G^o}{RT}\right) = K \qquad (16)$$

Using Equation (16), the value of K for any reaction at a specific T can be estimated. Since the involved reactions can be determined, the $\left(\Delta G^o / RT\right)$ of any reaction can be estimated using Equation (17) [28].

$$\frac{\Delta G^o}{RT} = \frac{\Delta G_0^o - \Delta H_0^o}{RT_0} + \frac{\Delta H_0^o}{RT} + \frac{1}{T}\int_{T_0}^{T} \frac{\Delta C_P^o}{R} dT - \int_{T_0}^{T} \frac{\Delta C_P^o}{R} \frac{dT}{T} \qquad (17)$$

Assuming that the reaction takes place in a gas phase, the relation of the fugacity and fugacity coefficient at a certain P can be written as Equation (18),

$$\hat{f}_i = \hat{\phi}_i y_i P \qquad (18)$$

where, $\hat{\phi}_i$ and y_i stand for the fugacity coefficient and mole fraction of species i, respectively. At low pressure and/or a high temperature, the system can be considered to be ideal gas mixtures or ideal solutions [29], so that the fugacity is equal to its pressure, $f_i^o = P^o$, for each species i. Substituting Equation (18) to Equation (16) and applying the mentioned assumption obtain the relation of the equilibrium constant to the composition and pressure as written as Equation (19),

$$\prod_i \left(y_i \hat{\phi}_i\right)^{v_i} = \left(\frac{P}{P^o}\right)^{-v} K \qquad (19)$$

where, $v = \sum_i v_i$. If the equilibrium mixture is assumed to be an ideal solution and ideal gas mixture, the fugacity coefficient of species i is equal to 1 ($\hat{\phi}_i = 1$). Furthermore, the equilibrium composition can be estimated using Equation (19), since the equilibrium constant, K, can be estimated using Equation (16). Since the equilibrium composition can be estimated, the equilibrium conversion and yield can also be predicted using the following equations:

$$X_i\,(\%) = \frac{N_{i,in} - N_{i,out}}{N_{i,in}} \times 100 \qquad (20)$$

$$Y_i\,(\%) = \frac{N_i}{N_{feed}} \times 100 \qquad (21)$$

where X_i stands for the equilibrium conversion of species i, Y_i stands for the equilibrium yield of species i, N_i stands for total mol of species i, and N_{feed} is the total mole of reactants fed. The equilibrium yield of species is estimated based on the reactants fed to the reaction system. In the hydrodeoxygenation reaction, N_{feed} is the total mole of palmitic acid and hydrogen fed.

2.3 Reaction Models

Four models are investigated in this study. Table 1 shows the brief information of the reaction models. The first model (Model I) illustrates the deoxygenation of palmitic acid in which the external hydrogen gas is introduced to the reaction system. In Model II, the feasibility study is focused on the decarboxylation and decarbonylation reactions of palmitic acid. This model let us know the feasibility of the main reaction pathways of hydrogen-free deoxygenation, namely decarboxylation and decarbonylation reactions. Furthermore, Model III includes the WGS reaction. With this Model III, we can investigate the formation of internal hydrogen gas in the hydrogen-free deoxygenation. Finally, Model IV considers the possibility of hydrodeoxygenation pathways, since the internal hydrogen can be generated.

Table 1. Reaction models considered in this study.

Model	Reaction pathways	Reaction condition
Model I	Equations (1) – (9)	Hydrodeoxygenation with external hydrogen (H_2/Palmitic acid ratio = 0 – 20)
Model II	Equations (1) and (2)	Hydrogen-free deoxygenation (decarboxylation and decarbonylation) without external hydrogen
Model III	Equations (1), (2) and (5)	Hydrogen-free deoxygenation (decarboxylation and decarbonylation) and WGS reactions without external hydrogen
Model IV	Equations (1) – (9)	Deoxygenation with internal hydrogen generation (internal hydrodeoxygenation)

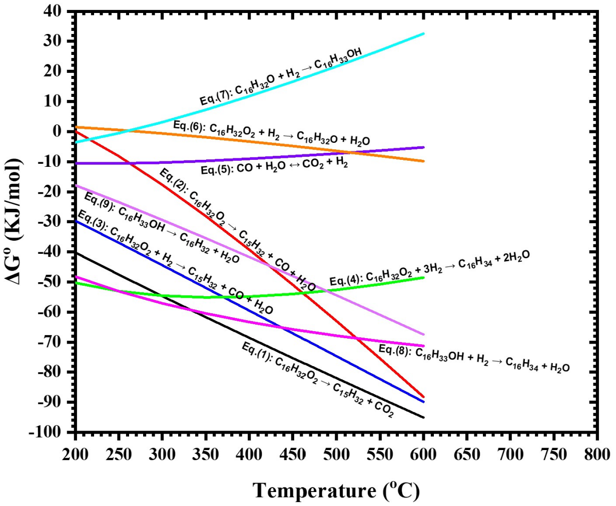

Figure 1. The standard Gibbs-energy change of reaction (ΔG°) at various reaction temperatures.

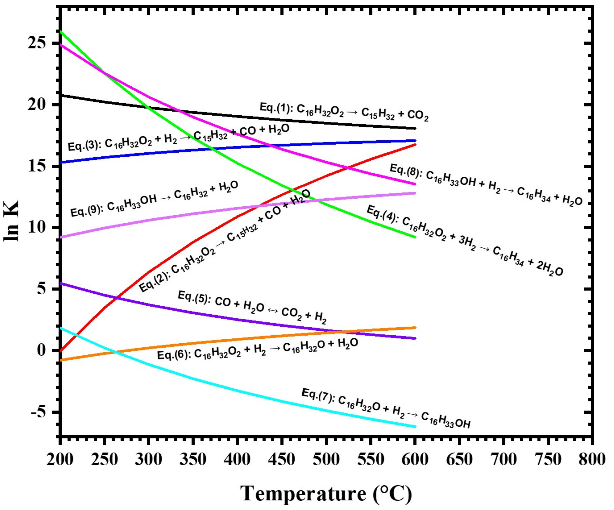

Figure 2. The equilibrium constant (*K*) of reaction at various reaction temperatures.

3.0 RESULTS AND DISCUSSION

3.1 Feasibility Analysis of Deoxygenation-Decarbonylation Reactions through Standard Gibbs-energy Change of Reaction

The feasibility analysis of the deoxygenation-decarbonylation reactions can be observed through the standard Gibbs-energy change of reaction (Δ*G*°). Basically, the standard Gibbs-energy change of a reaction is estimated through the difference between the standard Gibbs energy of the formation of products and reactants or $\sum_i v_i G_i^o$. However, it can be estimated using Equation (17) as a function of reaction temperature. It is known that the Δ*G*° acts as the thermodynamic driving force of reaction, because the value of Δ*G*° determines the equilibrium constant, as shown in Equation (16). If the Δ*G*° is positive, the reaction is difficult to be conducted, because the value of the equilibrium constant is low. Inversely, if the Δ*G*° is negative, the reaction is easy to be performed, because the value of the equilibrium constant is high [29]. Figure 1 shows the standard Gibbs-energy change (Δ*G*°) of all possible deoxygenation-decarbonylation reactions at various reaction temperatures, while the value of reaction equilibrium constants (as ln *K*) is presented in Figure 2.

As observed in Figure 1, the values of Δ*G*° for both hydrogen-assisted (Equations (3) and (4)) and hydrogen-free (Equations (1) and (2)) deoxygenation reactions are negative. It confirms that both reaction mechanisms are thermodynamically favorable to occur. Richardson [30] has classified the criteria for thermodynamic feasibility of chemical reaction according to the standard Gibbs-energy change of reaction, namely very negative (< −41.48 kJ/mol), moderately negative (0 to −41.48 kJ/mol), moderately positive (0 to 41.48 kJ/mol), and highly positive (>41.48 kJ/mol). According to these criteria, hydrogen-free deoxygenations (Equations (1) and (2)) and hydrogen-assisted deoxygenations (Equations (3) and (4)) are very negative, meaning possibly producing a very high equilibrium conversion of palmitic acid. Interestingly, the hydrogen-free deoxygenation of palmitic acid is thermodynamically more favorable than the hydrodeoxygenation (Equations (3) and (4)), because the standard Gibbs-energy change of this reaction is more negative than the hydrogen-assisted deoxygenation. It means that it is thermodynamically possible to carry out the deoxygenation reactions (Equations (1) and (2) and/or (5)) of palmitic acid without external hydrogen gas addition.

Concerning the hydrogen-free deoxygenation reaction, the palmitic acid can be deoxygenated to hydrocarbons through decarboxylation, releasing CO_2 (Equation (1)) and decarbonylation, releasing CO dan H_2O (Equation (2)). As can be seen in Figure 1, at lower temperatures (≤200 °C), the Δ*G*° of the decarbonylation reaction is moderately positive, meaning that it has low equilibrium conversions at low temperatures (except for Equation (1) of decarboxylation). Therefore, it is reasonable to point out that the decarboxylation reaction is thermodynamically more favorable than the decarbonylation reaction at lower reaction temperature. However, the decarbonylation reaction is more favorable at higher reaction temperatures than the decarboxylation reaction. Consequently, CO and H_2O reaction products may be further converted slightly into H_2 and CO_2 through the water gas shift (WGS) reaction (Equation (5)). As can be seen in Figure 1, the WGS reaction has moderately negative Δ*G*°, which possibly gives fairly high equilibrium conversions [30]. Therefore, it can be advised that generating in situ or internal hydrogen during the hydrogen-free deoxygenation reaction through the WGS reaction is possible, although it is not favorable at higher reaction temperature.

With the presence of H_2 gas in the reaction system, hydrodeoxygenation reactions of palmitic acid (Equations (3) and (4)) are possibly favored, even without addition of external hydrogen gas. One mole palmitic acid can react with three moles H_2, producing one-mole n-hexadecane and two moles H_2O (Equation (4). Since this reaction (Equation (4)) has very negative Δ*G*°, it is reasonable to suggest that the hydrodeoxygenation reaction is thermodynamically favorable as the presence of (external and/or internal) H_2 gas. It was also reported that this reaction might occur through the formation of intermediates species, namely aldehyde and alcohol [16]. In this case, the palmitic acid is hydrogenated into hexadecanal (Equation (6)) and further hydrogenated into hexadecanol (Equation (7)). Furthermore, the hexadecanol is further hydrogenated into n-hexadecane (Equation (8)) or further dehydrated into 1-hexadecene (Equation (9)). As can be seen in Figure 1, the hydrogenation of palmitic acid to hexadecanal (Equation (6)) is thermodynamically more favorable than that of hexadecanal to hexadecanol (Equation (7)), especially at higher reaction temperature. Therefore, it is possible to obtain more hexadecanal than hexadecanol in the reaction product. As comparison, Duan *et al.* [27] reported that hexadecanal and hexadecanol were formed as the intermediates of palmitic acid hydrodeoxygenation.

As comprehensively explained, through the feasibility analysis of reactions using the standard Gibbs-energy change of reactions thermodynamically, it is reasonable to conclude that it is possible to carry out the hydrogen-free deoxygenation reaction of palmitic acid to hydrocarbons. Meanwhile, the hydrogen gas can also be generated through the WGS reaction, which can initiate the occurrence of hydrodeoxygenation of palmitic acid, even though there is no external hydrogen gas addition. Although the reactions are thermodynamically favorable, the reactions might occur more favorable if atoms and electrons of the reactants were given the opportunity to rearrange into products at lower activation energy, which should be supported by a catalyst.

3.2 Hydrodeoxygenation Reaction of Palmitic Acid (Model I)

In this section, the deoxygenation of palmitic acid is focused on the hydrogen-assisted deoxygenation. The thermodynamic analysis of hydrodeoxygenation reaction was conducted to compare with hydrogen-free deoxygenation, which is discussed in the next section. Model I include all proposed reactions, in which some reactions require hydrogen gas. Hence, it is suggested that the hydrogen gas concentration in the feed for this model should influence the equilibrium composition. Therefore, the hydrogen gas concentration in the feed, expressed as the mole ratio of hydrogen to palmitic acid, is discussed. In addition, some parameters, including reaction temperature and pressure, are also assessed in this section.

Figure 3 shows the effect of hydrogen gas concentration in feed on equilibrium conversions and product compositions at reaction temperature of 350 °C and reaction pressure of 1 bar which is calculated using Equation (19). As can be observed in Figure 3(A), the equilibrium conversion of palmitic acid is nearly complete at all H_2/Palmitic acid ratios. It indicates that the palmitic acid can be completely converted at all H_2/Palmitic acid ratio ranges. A different trend is found for hydrogen conversion. The equilibrium conversion of hydrogen tends to decrease as the increase of hydrogen concentration. It is highly suggested that the increase in hydrogen concentration gives more excessive concentration in the reaction system. As the hydrogen becomes the excess reactant, the equilibrium conversion of hydrogen decreases [20]. Figure 3(B) shows that the equilibrium composition varies according to H_2/Palmitic acid ratio. As the H_2/Palmitic acid ratio increases from 0 to 10, the equilibrium composition of H_2 increases due to the excessive effect of H_2. Meanwhile, in the absence of hydrogen (H_2/Palmitic acid ratio = 0), the main components are $C_{15}H_{32}$ and CO_2, which are produced from the decarboxylation reaction pathway. However, as the hydrogen concentration increases, the formation of $C_{15}H_{32}$ and CO_2 decreases. On the other hand, the reaction favors the formation of $C_{16}H_{34}$ due to the hydrogenation reaction.

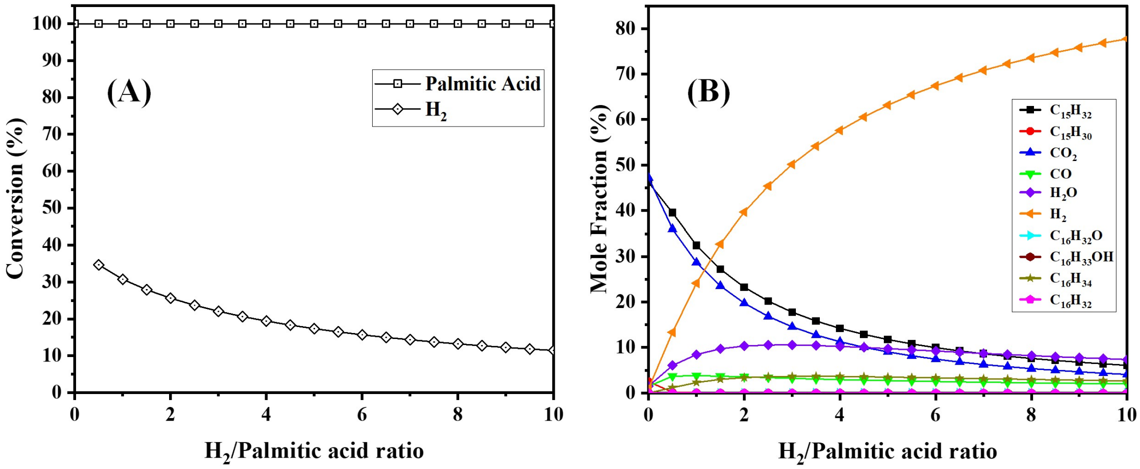

Figure 3. Effect of H_2/Palmitic acid ratio on equilibrium (A) conversions and (B) product composition for Model I (*P* = 1 bar, *T* = 350 °C).

Figure 4 shows the effect of temperature on the equilibrium conversion of palmitic acid and hydrogen as well as the product composition with an H_2/Palmitic acid ratio of 3 at 1 bar. This ratio was used in this study, because it is the stoichiometric ratio that is required to remove oxygen in palmitic acid as water (Equation (4) or briefly explained as Equations (6) – (8)). As can be seen in Figure 4(A), the equilibrium conversion of palmitic acid is highly close to 100% at all reaction temperatures. On the other hand, hydrogen conversion decreases monotonically until 400 °C from 71.36% to 15.39% and then constant for ~14% at 425–475 °C. With a further increase in reaction temperature, the equilibrium conversion of hydrogen decreases to 1.71% at 600 °C. The first decrease in the hydrogen conversion at 200–400 °C is caused by the decrease in hydrodeoxygenation reaction selectivity as the reaction temperature increases. The hydrodeoxygenation of palmitic acid is a highly exothermic reaction; therefore, it is unfavorable at high temperatures. As can be seen in Figure 4(B), the equilibrium composition of $C_{16}H_{34}$ decreases from 19.96% to 1.05% at 400 °C and becomes negligible at further higher temperatures. The constant and further decrease in the conversion of the hydrogen is attributed to the formation of hydrogen through WGS reaction, since CO and H_2O are produced through endothermic decarbonylation (Equation (2)) and hydro-decarbonylation (Equation (3)). Even though the WGS reaction is exothermic, which should be unfavorable at high temperatures, the equilibrium of this reaction is expected to be shifted to the right or toward product formation, since the composition of CO and H_2O are highly produced by the favorable decarbonylation and hydro-decarbonylation reactions, according to Le Chatelier's principles.

As shown in Figure 4(B), at 200 °C, the product mainly contains H_2O, $C_{16}H_{34}$, H_2, $C_{15}H_{32}$ and CO_2 indicating that the main-occurred reaction pathways are hydrodeoxygenation and decarboxylation of palmitic acid. It is true, since the ratio of H_2O and $C_{16}H_{34}$, as well as the ratio of $C_{15}H_{32}$ and CO_2, are equal to their stoichiometric ratio (see Equations (1) and (4)). However, it is found that the equilibrium composition, or can be addressed as product selectivity, of $C_{16}H_{34}$ decreases from 19.96% to 1.05% at 400 °C, which is accompanied by the decrease in H_2O. It is caused by the fact that the hydrodeoxygenation reaction of palmitic acid is an exothermic reaction making it thermodynamically unfavorable at a high reaction temperature. It was postulated that increasing the reaction temperature could decrease the value of the equilibrium constant of an exothermic reaction causing a shift of the reaction equilibrium toward reactants [28]. On the other hand, the decarboxylation reaction becomes more favorable at a higher temperature. The selectivity of $C_{15}H_{32}$ increases with the increase in reaction temperature. However, it is expected to be unfavorable at reaction temperatures around 300 – 350 °C, since the selectivity of CO_2 is found to be maximum at this reaction temperature range, which is mainly produced through decarboxylation reaction rather than through WGS reaction. However, the selectivity of $C_{15}H_{32}$ still increases and becomes optimum at around 400 – 450 °C due to the favorable hydro-decarbonylation reaction. Further increases in reaction temperature favor the decarbonylation reaction as indicated by the formation of $C_{15}H_{30}$.

The effect of pressure on equilibrium conversions and product composition at 350 °C and an H_2/Palmitic acid ratio of 3 is depicted in Figure 5. As can be seen, the palmitic acid can be completely converted close to 100% as the equilibrium conversion. Figure 5(A) shows that the equilibrium conversion of palmitic acid is not affected by reaction pressure, except for hydrogen conversion, which is highly affected by pressure. As can be seen, the equilibrium conversion of hydrogen increases as the increase in reaction pressure. The effect of reaction pressure on the reaction equilibrium can be explained by considering Equation (19). In this model, hydrogen is consumed in the hydro-decarbonylation (Equation (3)) and mainly in the hydrodeoxygenation reaction (Equation (4) or briefly explained as Equations (6)–(8)). As can be seen, the total stoichiometric number of hydrodeoxygenation reaction is negative; therefore, the reaction equilibrium shifts toward products, so that the conversion of hydrogen increases.

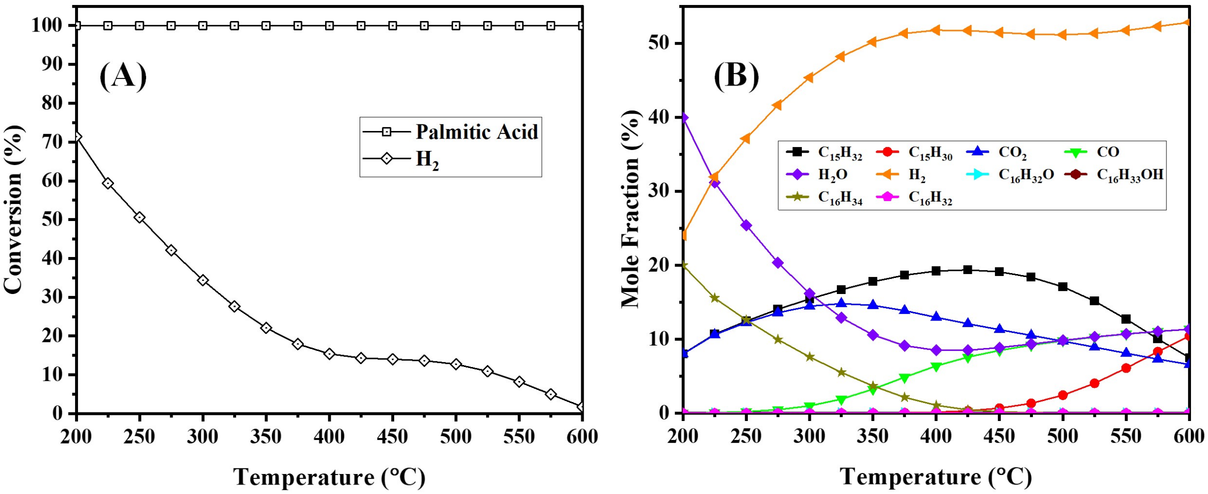

Figure 4. Effect of reaction temperature on (A) equilibrium conversions and (B) product composition for Model I (P = 1 bar, H_2/Palmitic acid = 3).

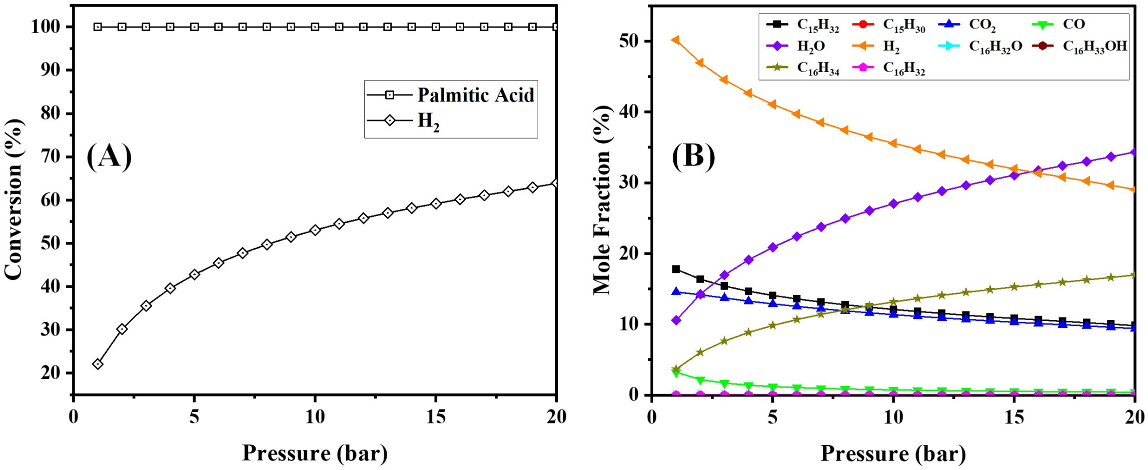

Figure 5. Effect of reaction pressure on (A) equilibrium conversions and (B) product composition for Model I (T = 350 °C, H_2/Palmitic acid = 3).

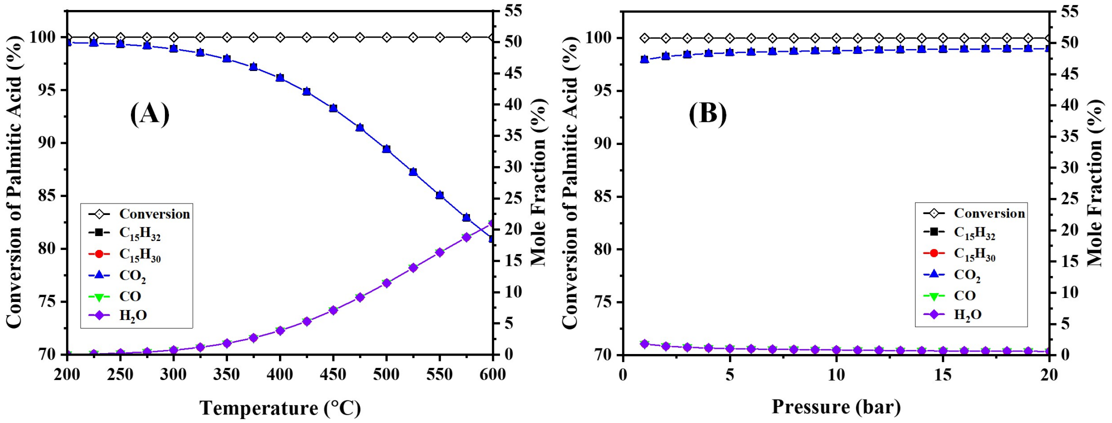

Figure 6. Effect of (A) reaction temperature and (B) reaction pressure on equilibrium conversions and product composition for Model II.

As shown in Figure 5(B), the reaction pressure affects the product composition. At equilibrium, the mole fraction of $C_{16}H_{34}$ increases from 3.67% to 16.97% as the increase in pressure from 1 to 20 bar. It indicates that the hydrodeoxygenation reaction is thermodynamically favorable at high reaction pressure. It is true, since the ratio of H_2O to $C_{16}H_{34}$ becomes close to 2 at higher reaction pressure. As shown in Figure 5(B), the mole fraction of H_2O increases with the pressure increases, while the ratio of H_2O to $C_{16}H_{34}$ decreases from 2.88 to 2.02, indicating that the hydrodeoxygenation reaction is thermodynamically more favorable than the others. The total stoichiometric number of hydrodeoxygenation reaction is negative, while the others are positive, so that the mole fractions of H_2O and $C_{16}H_{34}$ increase, while the others decrease.

3.3 Hydrogen-free Deoxygenation Reaction of Palmitic Acid

3.3.1 Model II (Equations (1) and (2) without Additional External Hydrogen)

In Model II, the study is focused on the two main reactions of hydrogen-free deoxygenation of palmitic acid, namely decarboxylation (Equation (1)) and decarbonylation (Equation (2)) reactions. In the decarboxylation reaction, the palmitic acid is converted into saturated hydrocarbon, namely pentadecane ($C_{15}H_{32}$), and CO_2. On the other hand, in the decarbonylation reaction, the palmitic acid is converted into an unsaturated hydrocarbon, namely 1-pentadecene ($C_{15}H_{30}$), CO, and H_2O. Figure 6 illustrates the effect of reaction pressure and reaction temperature on the equilibrium conversion of palmitic acid and the equilibrium of products composition.

As depicted in Figure 6(B), the reaction pressure does not affect the equilibrium conversion of palmitic acid at 350 °C. However, it can be deduced that palmitic acid can be completely converted into hydrocarbons, since the equilibrium conversion of palmitic acid is close to 100% at all studied reaction pressures (1 – 20 bar). In addition, this fact confirms that palmitic acid can be converted into hydrocarbons even though there is no addition of external hydrogen gas introduction. Furthermore, the equilibrium products composition is not also affected by reaction pressure. As seen in Figure 6(B), the composition of the product remains constant as the increase in reaction pressure. This confirms that the equilibrium composition or products selectivity of hydrogen-free deoxygenation of palmitic acid is not affected by the change in reaction pressure, which is different with Model I, where the product selectivity of Model I reactions is affected by reaction pressure.

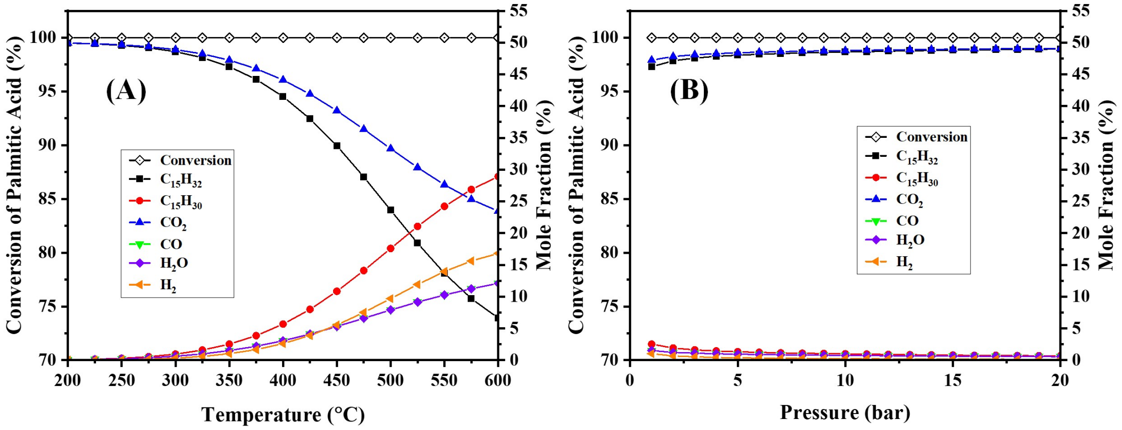

Figure 7. Effect of (A) reaction temperature and (B) reaction pressure on equilibrium conversions and product composition for Model III.

Similar to the effect of reaction pressure, the equilibrium conversion of palmitic acid is not affected by reaction temperature. At 1 bar reaction pressure, it is found that the palmitic acid can be completely converted to the reaction products, as the equilibrium conversion of palmitic acid is close to 100% at all temperatures (200 – 600 °C). Even though the reaction temperature has no effect on the palmitic acid conversion, it is found that the composition of the reaction product is highly affected by reaction temperature. As can be seen in Figure 6(A), at low reaction temperatures (<300 °C), the reaction product mainly consists of $C_{15}H_{32}$ and CO_2. It indicates that the decarboxylation reaction of palmitic acid is thermodynamically more favorable than that at low temperatures. It is true, since the decarboxylation reaction is an exothermic reaction which is thermodynamically more favorable at lower temperature. Furthermore, the mole fractions of $C_{15}H_{32}$ and CO_2 decrease as the reaction temperature increases. Otherwise, the mole fractions of $C_{15}H_{30}$, CO, and H_2O increase with the reaction temperature. The mole fraction of $C_{15}H_{32}$ seems to be constant (~49%) at <300 °C and rapidly decreases to 18.48% at 600°C. Below 300 °C, the selectivity of decarbonylation products is neglectable (<1%) and increases to 21.02% at 600 °C. The unsaturated hydrocarbon ($C_{15}H_{30}$) is rapidly produced through decarbonylation reaction after 300 °C. It is believed that the unsaturated hydrocarbons can be further converted into aromatic compounds and coke through the dehydrogenation reaction [31]. The decarbonylation reaction is more favorable at high reaction temperatures producing CO and H_2O, which converted to hydrogen through the WGS reaction.

3.3.2 Model III (Equations (1), (2), and (5) without Additional External Hydrogen)

As explained previously in Section 3.3.1, it is found that the decarboxylation reaction (Equation (1)) of palmitic acid is more favorable at low reaction temperatures, while the decarbonylation reaction (Equation (2)) is more favorable at high reaction temperatures. As the decarbonylation reaction is more favorable, the production of CO and H_2O increases. It is well-known that these components are the reactant of the WGS reaction (Equation (5)). Through the WGS reaction, internal hydrogen (H_2) can be formed, which further can promote the hydrodeoxygenation reaction. In this model (III), the WGS reaction is included in the feasibility study of internal hydrogen formation in the hydrogen-free deoxygenation of palmitic acid.

Figure 7 depicts the effect of reaction temperature and reaction pressure on the equilibrium conversions of palmitic acid and equilibrium products composition or selectivity. As can be seen in Figure 7(A), the reaction temperature does not affect the equilibrium conversion of palmitic acid in this Model III, which remains constant at 100%. Since this model (III) includes the WGS reaction and the equilibrium conversion of palmitic acid is similar to Model II; therefore, it can be deduced that the conversion of palmitic acid is not affected by the presence of the WGS reaction. However, the equilibrium composition is highly affected by reaction temperature. It is found that the WGS reaction occurs producing H_2 with the equilibrium selectivity of 0.01% at 200 °C. It indicates that the WGS reaction is favorable even at low temperatures, since the WGS reaction is an exothermic reaction. The formation of H_2 increases with temperature. It is interesting that the WGS reaction is an exothermic reaction which should be unfavorable at high temperatures. However, the equilibrium of the WGS reaction is shifted toward reaction products, because the reactants species (CO and H_2O) are highly produced at higher temperatures through the decarbonylation reaction. Based on Le Chatelier's principle, the reaction equilibrium shifts toward products if the reactants are much provided. Therefore, this model suggests that internal hydrogen (H_2) used for hydrodeoxygenation can be produced through the WGS reaction at high reaction temperatures.

Concerning the hydrocarbons formation, it can be seen that the equilibrium selectivity profiles of $C_{15}H_{32}$ and $C_{15}H_{30}$ in this Model (III) are similar to those in Model II. As the increase in reaction temperature from 200 to 300 °C, the selectivity of $C_{15}H_{32}$ slightly decreases and thus rapidly decreases at a further higher temperature. On the contrary, the selectivity of $C_{15}H_{30}$ rapidly increases from 1.58% at 325 °C to 28.91% at 600 °C. Even though the equilibrium selectivity profiles of hydrocarbons are similar, the equilibrium selectivity of $C_{15}H_{32}$ in Model III is lower than that in Model II, while the equilibrium selectivity of $C_{15}H_{30}$ is higher than Model II. It indicates that the equilibrium reaction is shifted toward unsaturated hydrocarbon formation through decarbonylation reaction because of the presence of the WGS reaction. The WGS reaction consumes CO and H_2O, the products of decarbonylation reaction, to produce

H_2 (internal hydrogen) and CO_2 that used for hydrodeoxygenation reaction. Since those species (CO and H_2O) are consumed in the WGS reaction, the equilibrium of decarbonylation reaction is shifted toward products. On the other hand, CO_2 gas is the product of decarboxylation and WGS reactions. The formation of CO_2 gas through the WGS reaction affects the decarboxylation reaction as CO_2 becomes abundant availability. As a result, the reaction equilibrium of decarboxylation shifts towards reaction and the equilibrium selectivity of $C_{15}H_{32}$ decreases.

With respect to the effect of reaction pressure on the equilibrium conversion (Figure 7(B)), the equilibrium conversion of palmitic acid and the equilibrium composition of products of Model III are not affected by reaction pressure. On the comparison between this model (Model III) to Model II (section 3.3.1), this model III includes the WGS reaction, which is not affected by reaction pressure, because of the null total stoichiometric number of the WGS reaction. However, the effect of reaction pressure in this model III is supposed to be the same as in Model II.

3.3.3 Model IV (All Possible Reactions in Equations (1)-(9))

As reported in Section 3.3.2, the internal hydrogen (H_2 produced from WGS reaction) is expected to support hydrogenation in the hydrodeoxygenation and hydro-decarbonylation reactions of palmitic acid. In this section, model IV includes hydrodeoxygenation and hydro-decarbonylation reactions to study the feasibility of those reactions in the external hydrogen-free (use internal hydrogen) deoxygenation of palmitic acid. Even, the reactions of hydrodeoxygenation and hydro-decarbonylation can increase the heating value of biofuels, because the number of C and H in biofuels becomes high [20].

Figure 8 shows the effect of reactions temperature and pressure on equilibrium conversion and products composition for Model IV. The equilibrium conversion of palmitic acid is not affected by the reaction temperature (Figure 8(A)) in Model IV, which is similar to the previous model (Model III). It indicates that the equilibrium conversion of palmitic acid in the hydrogen-free deoxygenation (internal hydrogen present) is not affected by the reaction pathways. However, the reaction temperature affects the equilibrium composition of products in Model IV. As shown in Figure 8(A**)**, the selectivity profiles of $C_{15}H_{32}$, $C_{15}H_{30}$, CO_2, CO, H_2O, and H_2 are similar to those in Model III. At reaction temperature T < 300 °C, the decarboxylation reaction is the most thermodynamically favorable due to an exothermic reaction. On the contrary as reaction temperature increases, the decarbonylation and WGS reactions are more thermodynamically favorable than the decarboxylation reaction. It is true, since the decarbonylation reaction is an endothermic reaction. Even though the WGS reaction is exothermic, it is still favorable at higher temperatures, because the reactants (CO and H_2O) are highly produced through a favorable decarbonylation reaction.

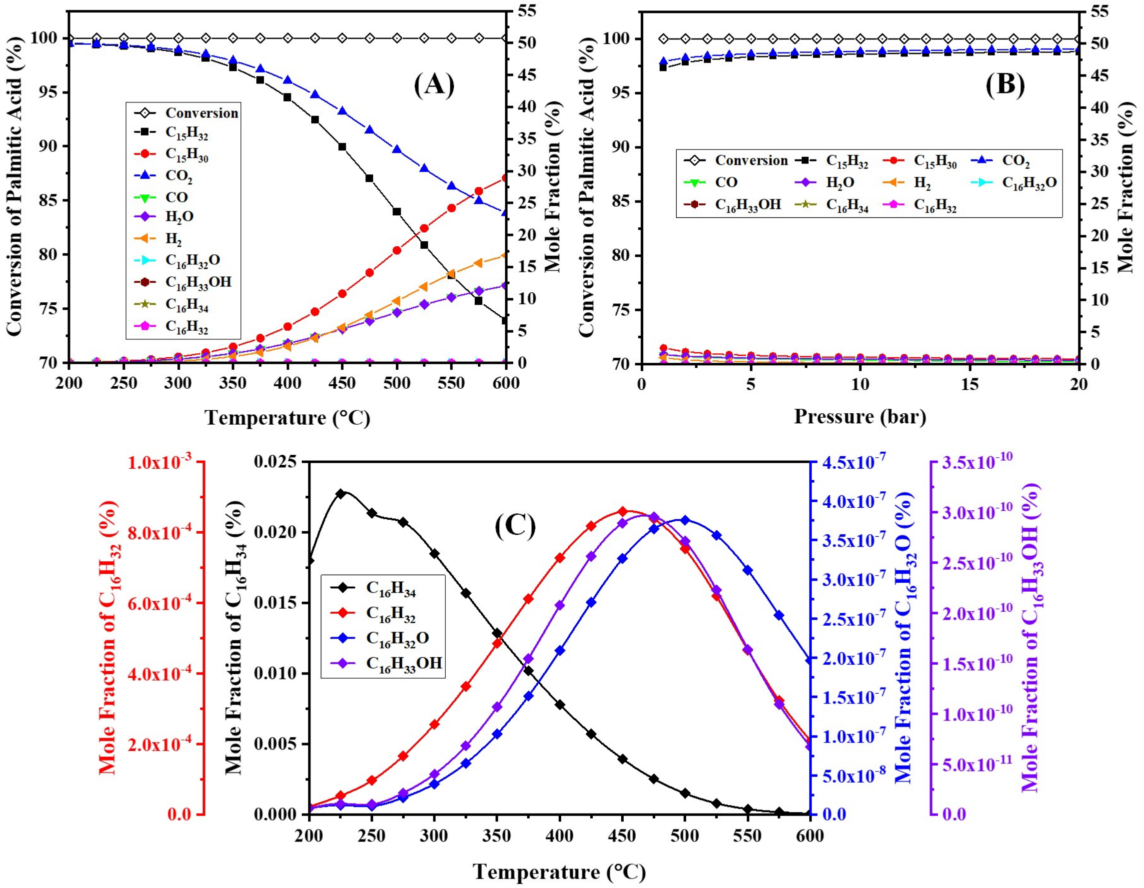

Figure 8. Effect of (A) reaction temperature and (B) reaction pressure on equilibrium conversions and products composition and (C) effect of reaction temperature on equilibrium composition of C_{16}-hydrocarbons and intermediate species for Model IV.

Concerning the formation of higher hydrocarbons ($C_{16}H_{34}$ and $C_{16}H_{32}$) and the intermediate species ($C_{16}H_{32}O$ and $C_{16}H_{33}OH$), the involved reactions are not too favorable, although H_2 is provided by the WGS reaction (internal hydrogen present). As shown in Figure 8(C), the equilibrium selectivity of those species is low and negligible. The highest equilibrium selectivity of $C_{16}H_{34}$, $C_{16}H_{32}$, $C_{16}H_{32}O$, and $C_{16}H_{33}OH$ is 0.023%, 8.59×10^{-4}%, 3.75×10^{-7}%, and 2.95×10^{-10}%, respectively. The equilibrium mole fraction or selectivity of $C_{16}H_{34}$ increases from 0.018% to 0.023% at 225 °C due to the low formation of H_2 at 200 °C, so the hydrodeoxygenation reaction is not favorable. However, it decreases at a further increase in temperatures due to the exothermic reaction behavior. With respect to the oxygenated products, it is shown that the composition of those components is negligible if the reaction is not kinetically controlled. However, it should be noted that some selective catalysts might lead to the formation of oxygenated products [22].

With respect to the effect of reaction pressure on the equilibrium conversion and products composition, it is shown in Figure 8(B) that the reaction pressure does not affect both equilibrium conversion of palmitic acid and the equilibrium selectivity or products composition. By the presence of a hydrodeoxygenation reaction (because the presence of internal hydrogen gas), it is supposed that this reaction can affect the equilibrium composition with respect to the reaction pressure. However, the hydrodeoxygenation reaction has no effect on the equilibrium product compositions since there is not enough internal hydrogen to support the hydrodeoxygenation reaction. Moreover, the highest internal hydrogen formation is favorable at higher reaction temperatures, which in turn assists progressing the unfavorable hydrodeoxygenation reaction thermodynamically.

3.4 Comparison of External Hydrogen-assisted and Hydrogen-free Deoxygenation of Palmitic Acid towards Hydrocarbons Formation

As mentioned before, the main hydrocarbons in the hydrogen-free deoxygenation models are C_{15}-hydrocarbons. Figure 9 shows the comparison of the equilibrium yield of the corresponding hydrocarbons for all models. The formation of C_{16}-hydrocarbons is considered in the Model IV via hydrodeoxygenation; however, it is found to be low and negligible. Concerning the formation of C_{15}-hydrocarbons, the equilibrium yield in Models III and IV seems to be equal. However, the formation of saturated hydrocarbon ($C_{15}H_{32}$) in Models III and IV is thermodynamically more unfavorable than in Model II. Inversely, the formation of unsaturated hydrocarbon ($C_{15}H_{30}$) in Models III and IV is thermodynamically more favorable than in Model II. This phenomenon occurs due to the presence of the WGS reaction which can shift forward the reaction equilibrium of the hydrogen-free deoxygenation of palmitic acid, following Le Chatelier's principle.

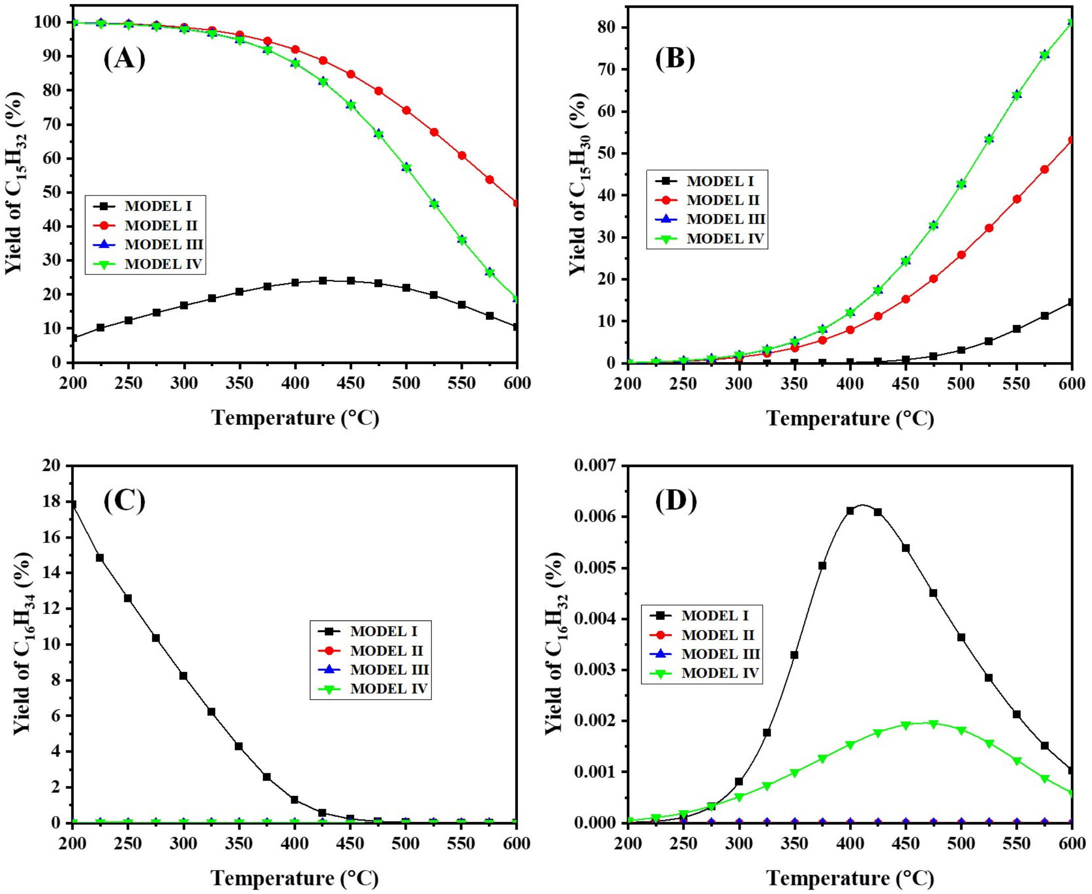

Figure 9. Equilibrium yield of (A) $C_{15}H_{32}$, (B) $C_{15}H_{30}$, (C) $C_{16}H_{32}$, and (D) $C_{16}H_{30}$ for all models.

Table 2. Comparison of hydrocarbon products distribution using thermodynamic equilibrium model and experimental data.

Temp. (°C)	**Conversion (%)**		**Hydrocarbon Selectivity (%)**					
			C_{15}		**C_{16}**		**≤ C_{14}**	
	Exp.	**Model I**	**Exp.**	**Model I**	**Exp.**	**Model I**	**Exp.**	**Model I**
240[a]	97.25	100	92.17	99.975	2.54	1.16×10^{-3}	5.49	-
260[b]	100	100	90	99.949	0.8	1.31×10^{-3}	9	-
270[c]	100	100	76	99.927	1.9	1.38×10^{-3}	22	-

[a] data taken from ref. [27]
[b] data taken from ref. [22]
[c] data taken from ref. [32]

The composition of biofuels product is expected to affect the heating value of the biofuels. In order to compare the heating value of the biofuels product, the higher heating value (HHV) of the biofuels can be estimated empirically. The HHV is estimated empirically using the following equation by Mateus *et al.* [32]:

$$HHV = 0.363302C + 1.087033H - 0.100992O \qquad (22)$$

where, HHV stands for the higher heating value (MJ/kg), while C, H, and O stand for the weight percent of C, H, and O atoms in the biofuels, respectively. Experimentally, these data can be obtained through an ultimate analysis. In this study, the weight percent of those atoms is predicted from the equilibrium composition of products, i.e. $C_{15}H_{30}$, $C_{15}H_{32}$, $C_{16}H_{32}$, $C_{16}H_{34}$, $C_{16}H_{32}O$, and $C_{16}H_{33}OH$. Equation (22) was developed to estimate the HHV for biomass-derived biofuels with low sulfuric content [33]. Therefore, this equation can be used to estimate the HHV of the biofuels product as presented in Figure 10. The figure depicts the estimated HHV of Model I and Model IV. Those models are used for comparison because they have the same reaction pathways. As can be seen, the estimated HHV of Model I and Model IV ranges from 46.78 – 47.25 MJ/kg. Moreover, the HHV of Model I is relatively higher than Model IV, because the estimated HHV is affected by the weight percent of C, H, and O atoms. In addition, the weight percent of H atom has more influence than the others. It was reported that the heating value increased with increasing the hydrogen content [34]. Therefore, the higher estimated HHV in Model I is attributed to the higher hydrogen atom in the biofuels, which is higher than Model IV. This is because of the introduction of external hydrogen gas to the reaction system in Model I, which can increase the hydrogen content in the biofuels. Even though Model IV has a lower HHV than Model I, it still shows a good result, since the estimated HHVs are not significantly different. Indeed, it can be concluded that the hydrogen-free deoxygenation (with only internal hydrogen) of palmitic acid can produce a comparable HHV with the hydrogen-assisted deoxygenation (with addition of external H_2 gas).

3.5 Case Study

The distribution of the hydrocarbon products using thermodynamic equilibrium model was compared with the experimental data. The data were obtained from literature. Indeed, the thermodynamic equilibrium selectivity is different with the experimental data. It should be known that the experimental data might not be in equilibrium state. However, the trend of selectivity from the experimental data should be in line with the thermodynamic equilibrium. As can be seen in Table 2, the experimental conversion of palmitic acid is close to 100% and approach the equilibrium conversion.

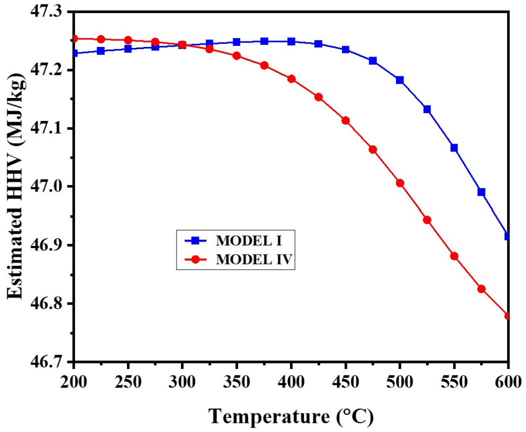

Figure 10. Estimated HHV for Model I and Model IV as a function of reaction temperature.

Based on the experimental data, the hydrocarbon selectivity mainly consists of C_{15} hydrocarbons (pentadecane and pentadecene). This is similar to the thermodynamic equilibrium model. It indicates that the main reaction is decarboxylation. As can also be seen in Table 2, the selectivity of C_{15} hydrocarbon decreases as the increase in the reaction temperature. It proves that the decarboxylation reaction is favored in low temperature. Even though the thermodynamic equilibrium model does not accurately predicted the hydrocarbon selectivity, it still can predict the trend of selectivity.

3.6 Recommendations for the Future Experimental Studies

As comprehensively discussed above, the pre-conclusion can be made that hydrogen-free deoxygenation (without additional external hydrogen gas) is thermodynamically favorable. If the saturated hydrocarbons are the main preferable product, it is recommended that the reaction should be conducted at lower reaction temperatures (<300 °C). In this case, the most favorable reaction is the decarboxylation reaction (Equation (1)) at lower temperatures, producing $C_{15}H_{32}$ (saturated) and CO_2. With respect to biofuels production, the saturated hydrocarbons products are mostly desired, because of their high combustion energy or HHV. In the experimental works point of view, the saturated hydrocarbons prevent condensation reaction, which can lead to aromatic compounds and coke formation [31]. It is possible to carry out the hydrogen-free deoxygenation at atmospheric reaction pressure. However, it should be noted that this recommendation is driven by the assumption that the reaction is not kinetically controlled. As comprehensively discussed, Model I and Model IV produce low equilibrium composition or negligible composition of the oxygenated products. However, some researchers reported that those oxygenated compounds were found in considerable quantities in the hydrodeoxygenation process [23,26,27]. Therefore, appropriate and selective heterogeneous catalysts should be implemented in the case of the catalytic reaction.

4.0 CONCLUSION

The hydrogen-free deoxygenation (without additional external hydrogen gas) of palmitic acid to hydrocarbons is thermodynamically favorable with almost complete conversion of the palmitic acid at studied reaction temperature range of 200–600 °C. The decarboxylation reaction is thermodynamically more favorable than the decarbonylation reaction at lower reaction temperature and showed inversely trend at higher reaction temperature. The equilibrium products composition is also highly affected by reaction temperature, in which at lower reaction temperatures, the main hydrocarbon product is saturated hydrocarbon ($C_{15}H_{32}$), while at higher reaction temperatures, the main hydrocarbon product is unsaturated hydrocarbon ($C_{15}H_{30}$). However, the equilibrium products composition is not affected by the reaction pressure, while in contrast, hydrodeoxygenation of palmitic acid is highly affected by reaction pressure. It is found that the internally generated hydrogen is thermodynamically favorable during the hydrogen-free deoxygenation, even at lower reaction temperature and not favorable at higher reaction temperature. Even though the internal hydrogen is possibly generated thermodynamically, the hydrodeoxygenation reaction pathways are not too favorable, since the hydrodeoxygenation product and its intermediates are found to be negligible.

Acknowledgement

The authors would like to express their sincere gratitude to the Ministry of Education, Culture, Research, and Technology, Republic of Indonesia, for the financial support through the research project of *Penelitian Disertasi Doktor* with contract number: 345-27/UN7.6.1/PP/2022.

References

[1] Zhou, G., Li, J., Yu, Y., Li, X., Wang, Y., Wang, W., Komarneni, S. 2014). Optimizing the distribution of aromatic products from catalytic fast pyrolysis of cellulose by ZSM-5 modification with boron and co-feeding of low-density polyethylene. *Applied Catalysis A: General*, 487: 45–53. DOI: 10.1016/j.apcata.2014.09.009.

[2] Ansari, K.B., Arora, J.S., Chew, J.W., Dauenhauer, P.J., Mushrif, S.H. 2019. Fast Pyrolysis of Cellulose, Hemicellulose, and Lignin: Effect of Operating Temperature on Bio-oil Yield and Composition and Insights into the Intrinsic Pyrolysis Chemistry. *Industrial and Engineering Chemistry Research*, 58(35): 15838–15852. DOI: 10.1021/acs.iecr.9b00920.

[3] Wulandari, N.M., Efiyanti, L., Trisunaryanti, W., Oktaviano, H.S., Bahri, S., Ni'mah, Y.L., Larasati, S. 2021. Effect of CTAB Ratio to the Characters of Mesoporous Silica Prepared from Rice Husk Ash in the Pyrolysis of a–cellulose. *Bulletin of Chemical Reaction Engineering & Catalysis*, 16(3): 632–640. DOI: 10.9767/bcrec.16.3.10828.632-640.

[4] Al-Muttaqii, M., Kurniawansyah, F., Prajitno, D.H., Roesyadi, A. 2019. Bio-kerosene and Bio-gasoil from Coconut Oils via Hydrocracking Process over Ni-Fe/HZSM-5 Catalyst. *Bulletin of Chemical Reaction Engineering & Catalysis*, 14(2): 309–319. DOI: 10.9767/bcrec.14.2.2669.309-319.

[5] Trisunaryanti, W., Triyono, T., Ghoni, M.A., Fatmawati, D.A., Mahayuwati, P.N., Suarsih, E. 2020. Hydrocracking of Calophyllum inophyllum Oil Employing Co and/or Mo Supported on γ-Al2O3 for Biofuel Production. *Bulletin of Chemical Reaction Engineering & Catalysis*, 15(3): 743–751. DOI: 10.9767/bcrec.15.3.8592.743-751.

[6] Paramesti, C., Trisunaryanti, W., Larasati, S., Santoso, N.R., Sudiono, S., Triyono, T., Fatmawati, D.A. 2021. The Influence of Metal Loading Amount on Ni/Mesoporous Silica Extracted from Lapindo Mud Templated by CTAB for Conversion of Waste Cooking Oil into Biofuel. *Bulletin of Chemical Reaction Engineering & Catalysis*, 16(1): 22–30. DOI: 10.9767/bcrec.16.1.9442.22-30.

[7] Wang, Q., Song, H., Pan, S., Dong, N., Wang, X., Sun, S. 2020. Initial pyrolysis mechanism and product formation of cellulose: An Experimental and Density functional theory(DFT) study. *Scientific Reports*, 10(1): 3626. DOI: 10.1038/s41598-020-60095-2.

[8] Riyanto, T., Istadi, I., Jongsomjit, B., Anggoro, D.D., Pratama, A.A., Al Faris, M.A. 2021. Improved Brønsted to Lewis (B/L) Ratio of Co- and Mo-Impregnated ZSM-5 Catalysts for Palm Oil Conversion to Hydrocarbon-Rich Biofuels. *Catalysts*, 11(11): 1286. DOI: 10.3390/catal11111286.

[9] Gurdeep Singh, H.K., Yusup, S., Quitain, A.T., Abdullah, B., Ameen, M., Sasaki, M., Kida, T., Cheah, K.W. 2020. Biogasoline production from linoleic acid via catalytic cracking over nickel and copper-doped ZSM-5 catalysts. *Environmental Research*, 186: 109616. DOI: 10.1016/j.envres.2020.109616.

[10] Mäki-Arvela, P., Kubickova, I., Snåre, M., Eränen, K., Murzin, D.Y. 2007. Catalytic Deoxygenation of Fatty Acids and Their Derivatives. *Energy & Fuels*, 21(1): 30–41. DOI: 10.1021/ef060455v.

[11] Hermida, L., Abdullah, A.Z., Mohamed, A.R. 2015. Deoxygenation of fatty acid to produce diesel-like hydrocarbons: A review of process conditions, reaction kinetics and mechanism. *Renewable and Sustainable Energy Reviews*, 42: 1223–1233. DOI: 10.1016/j.rser.2014.10.099.

[12] Krishnan, S.G., Pua, F.-L., Tan, E.-S. 2022. Synthesis of Magnetic Catalyst Derived from Oil Palm Empty Fruit Bunch for Esterification of Oleic Acid: An Optimization Study. *Bulletin of Chemical Reaction Engineering & Catalysis*, 17(1): 65–77. DOI: 10.9767/bcrec.17.1.12392.65-77.

[13] Mohammed, I.Y., Abakr, Y.A., Yusup, S., Alaba, P.A., Morris, K.I., Sani, Y.M., Kazi, F.K. 2017. Upgrading of Napier grass pyrolytic oil using microporous and hierarchical mesoporous zeolites: Products distribution, composition and reaction pathways. *Journal of Cleaner Production*, 162: 817–829. DOI: 10.1016/j.jclepro.2017.06.105.

[14] Palizdar, A., Sadrameli, S.M. 2020. Catalytic upgrading of biomass pyrolysis oil over tailored hierarchical MFI zeolite: Effect of porosity enhancement and porosity-acidity interaction on deoxygenation reactions. *Renewable Energy*, 148: 674–688. DOI: 10.1016/j.renene.2019.10.155.

[15] Sowe, M.S., Lestari, A.R., Novitasari, E., Masruri, M., Ulfa, S.M. 2022. The Production of Green Diesel Rich Pentadecane (C15) from Catalytic Hydrodeoxygenation of Waste Cooking Oil using Ni/Al2O3-ZrO2 and Ni/SiO2-ZrO2. *Bulletin of Chemical Reaction Engineering & Catalysis*, 17(1): 135–145. DOI: 10.9767/bcrec.17.1.12700.135-145.

[16] Istadi, I., Riyanto, T., Khofiyanida, E., Buchori, L., Anggoro, D.D., Sumantri, I., Putro, B.H.S., Firnanda, A.S. 2021. Low-oxygenated biofuels production from palm oil through hydrocracking process using the enhanced Spent RFCC catalysts. *Bioresource Technology Reports*, 14: 100677. DOI: 10.1016/j.biteb.2021.100677.

[17] Loe, R., Santillan-Jimenez, E., Morgan, T., Sewell, L., Ji, Y., Jones, S., Isaacs, M.A., Lee, A.F., Crocker, M. 2016. Effect of Cu and Sn promotion on the catalytic deoxygenation of model and algal lipids to fuel-like hydrocarbons over supported Ni catalysts. *Applied Catalysis B: Environmental*, 191: 147–156. DOI: 10.1016/j.apcatb.2016.03.025.

[18] Loe, R., Huff, K., Walli, M., Morgan, T., Qian, D., Pace, R., Song, Y., Isaacs, M., Santillan-Jimenez, E., Crocker, M. 2019. Effect of Pt Promotion on the Ni-Catalyzed Deoxygenation of Tristearin to Fuel-Like Hydrocarbons. *Catalysts*, 9(2): 200. DOI: 10.3390/catal9020200.

[19] Lestari, S., Mäki-Arvela, P., Simakova, I., Beltramini, J., Lu, G.Q.M., Murzin, D.Y. 2009. Catalytic Deoxygenation of Stearic Acid and Palmitic Acid in Semibatch Mode. *Catalysis Letters*, 130(1–2): 48–51. DOI: 10.1007/s10562-009-9889-y.

[20] Sahebdelfar, S., Ravanchi, M.T. 2017. Deoxygenation of propionic acid: Thermodynamic equilibrium analysis of upgrading a bio-oil model compound. *Renewable Energy*, 114: 1113–1122. DOI: 10.1016/j.renene.2017.07.100.

[21] Snåre, M., Kubičková, I., Mäki-Arvela, P., Eränen, K., Murzin, D.Y. 2006. Heterogeneous catalytic deoxygenation of stearic acid for production of biodiesel. *Industrial and Engineering Chemistry Research*, 45(16): 5708–5715. DOI: 10.1021/ie060334i.

[22] Peng, B., Zhao, C., Kasakov, S., Foraita, S., Lercher, J.A. 2013. Manipulating catalytic pathways: Deoxygenation of palmitic acid on multifunctional catalysts. *Chemistry - A European Journal*, 19(15): 4732–4741. DOI: 10.1002/chem.201203110.

[23] Ding, R., Wu, Y., Chen, Y., Liang, J., Liu, J., Yang, M. 2015. Effective hydrodeoxygenation of palmitic acid to diesel-like hydrocarbons over MoO2/CNTs catalyst. *Chemical Engineering Science*, 135: 517–525. DOI: 10.1016/j.ces.2014.10.024.

[24] Fang, X., Shi, Y., Wu, K., Liang, J., Wu, Y., Yang, M. 2017. Upgrading of palmitic acid over MOF catalysts in supercritical fluid of n-hexane. *RSC Advances*, 7(64): 40581–40590. DOI: 10.1039/c7ra07239b.

[25] Valencia, D., Conde, R.I., García, B., Ramírez-Verduzco, L.F., Aburto, J. (2020). Development of bio-inspired supports based on Ca–SiO2 and their use in hydrodeoxygenation of palmitic acid. *Renewable Energy*, 148: 1034–1040. DOI: 10.1016/j.renene.2019.10.087.

[26] Ding, R., Wu, Y., Chen, Y., Chen, H., Wang, J., Shi, Y., Yang, M. 2016. Catalytic hydrodeoxygenation of palmitic acid over a bifunctional Co-doped MoO2/CNTs catalyst: An insight into the promoting effect of cobalt. *Catalysis Science and Technology*, 6(7): 2065–2076. DOI: 10.1039/c5cy01575h.

[27] Duan, Y., Ding, R., Shi, Y., Fang, X., Hu, H., Yang, M., Wu, Y. 2017. Synthesis of Renewable Diesel Range Alkanes by Hydrodeoxygenation of Palmitic Acid over 5% Ni/CNTs under Mild Conditions. *Catalysts*, 7(12): 81. DOI: 10.3390/catal7030081.

[28] Smith, J.M., Van Ness, H.C., Abbott, M.M., Swihart, M.T. 2018. *Introduction to Chemical Engineering Thermodynamics*, 8th ed. New York, USA: McGraw-Hill Education.

[29] Istadi, I., Amin, N.A.S. 2005. Co-generation of C2 hydrocarbons and synthesis gases from methane and carbon dioxide: A thermodynamic analysis. *Journal of Natural Gas Chemistry*, 14(3): 140–150.

[30] Richardson, J.T. (1989). *Principles of Catalyst Development*, 1st ed. New York, USA: Springer.

[31] Rane, N., Kersbulck, M., van Santen, R.A., Hensen, E.J.M. 2008. Cracking of n-heptane over Brønsted acid sites and Lewis acid Ga sites in ZSM-5 zeolite. *Microporous and Mesoporous Materials*, 110(2–3): 279–291. DOI: 10.1016/j.micromeso.2007.06.014.

[32] Zhou, W., Xin, H., Yang, H., Du, X., Yang, R., Li, D., Hu, C. 2018. The Deoxygenation Pathways of Palmitic Acid into Hydrocarbons on Silica-Supported Ni12P5 and Ni2P Catalysts. *Catalysts*, 8(4): 153. DOI: 10.3390/catal8040153.

[33] Mateus, M.M., Bordado, J.M., Galhano dos Santos, R. 2021. Estimation of higher heating value (HHV) of bio-oils from thermochemical liquefaction by linear correlation. *Fuel*, 302: 121149. DOI: 10.1016/j.fuel.2021.121149.

[34] Demirbas, A. 2007. Effects of moisture and hydrogen content on the heating value of fuels. *Energy Sources, Part A: Recovery, Utilization and Environmental Effects*, 29(7): 649–655. DOI: 10.1080/009083190957801.